Received: 21 June 2016 | Accepted: 6 April 2017
DOI: 10.1002/hyp.11199

WILEY

RESEARCH ARTICLE

Assessment of spatial transferability of process-based hydrological model parameters in two neighbouring catchments in the Himalayan Region

Santosh Nepal[1] | **Wolfgang-Albert Flügel**[2] | **Peter Krause**[3] | **Manfred Fink**[2] | **Christian Fischer**[2]

[1] International Centre for Integrated Mountain Development (ICIMOD), GPO Box 3226, Kathmandu, Nepal

[2] Department of Geography, GI-Science Group, Friedrich-Schiller-University Jena, Jena, Germany

[3] Thuringian Environmental and Geological agency (TLUG), Jena, Germany

Correspondence
Santosh Nepal, International Centre for Integrated Mountain Development (ICIMOD), GPO Box 3226, Kathmandu, Nepal.
Email: santosh.nepal@icimod.org

Abstract

Estimating the hydrological regime of ungauged catchments in the Himalayan region is challenging due to a lack of sufficient monitoring stations. In this paper, the spatial transferability of the model parameters of the process-oriented J2000 hydrological model was investigated in 2 glaciated subcatchments of the Koshi river basin in eastern Nepal. The catchments have a high degree of similarity with respect to their static landscape features. The model was first calibrated (1986–1991) and validated (1992–1997) in the Dudh Koshi subcatchment. The calibrated and validated model parameters were then transferred to the nearby Tamor catchment (2001–2009). Sensitivity and uncertainty analyses were carried out for both subcatchments to discover the sensitivity range of the parameters in the two catchments. The model represented the overall hydrograph well in both subcatchments, including baseflow, rising and falling limbs; however, the peak flows were underestimated. The efficiency results according to both Nash–Sutcliffe (ENS) and the coefficient of determination (r^2) were above 0.84 in both catchments (1986–1997 in Dudh Koshi and 2001–2009 in Tamor). The ranking of the parameters in respect to their sensitivity matched well for both catchments while taking ENS and log Nash–Sutcliffe (LNS) efficiencies into account. However, there were some differences in sensitivity to ENS and LNS for moderately and less-sensitive parameters, although the majority (13 out of 16 for ENS and 16 out of 16 for LNS) had a sensitivity response in a similar range. The generalized uncertainty likelihood estimation results suggest that the parameter uncertainty are most of the time within the range and the ensemble mean matches very good (ENS: 0.84) with observed discharge. The results indicate that transfer of the J2000 parameters to a neighbouring catchment in the Himalayan region with similar physiographic landscape characteristics is viable. This indicates the possibility of applying a calibrated process-based J2000 model to other ungauged catchments in the Himalayan region, which could provide important insights into the hydrological system dynamics and provide much needed information to support water resources planning and management.

KEYWORDS

Dudh Koshi, Himalayan region, J2000 hydrological model, sensitivity and uncertainty analyses, Tamor, ungauged catchments

1 | INTRODUCTION

There are numerous ungauged catchments located in the mountainous headwater areas of the Himalayan region (Goswami, O'Connor, & Bhattarai, 2007). The remoteness and harsh mountain environment means that hydrometeorological stations are limited or absent and this applies especially for alpine and cryosphere headwater regions. But it is important to understand the hydrological regime such as high and low flows in these catchments (Singh, Mishra, & Chowdhary, 2001), both because of the huge potential for water resources development (Agrawala et al., 2003) and to gain a better basis for control and mitigation of extreme flooding encountered annually downstream. In addition, it is also important to understand current and future hydrological regime in the context of potential future climate change (Lutz et al., 2014; Nepal, 2016). Water resources assessment tools such as hydrological models can provide important information about the hydrological regime and can be instrumental for understanding runoff generation and concentration processes in ungauged catchments.

The role that hydrological models can play in different phases of planning and implementation of water resources development is well recognised (Anderson & Burt, 1985; DeCoursey, Shaake, & Seely, 1982; Kralisch, Krause, Fink, Fischer, & Flügel, 2007). Application of such models can provide vital information to support decision making in water management (Beven, 2001a, 2001b) as well as for basic research (Nepal, Krause, Flügel, Fink, & Fischer, 2014). However, the use of rainfall–runoff models to understand the hydrological regime in ungauged catchments is limited by the small number (or lack) of monitoring stations for hydrometeorological variables (Bárdossy, 2007; Blöschl, 2005; Bourgin, Andréassian, Perrin, & Oudin, 2015). Rainfall–runoff models have a number of calibration parameters that are difficult or impossible to estimate a priori either because they have no physical meaning or because of constraints in measuring these values with sufficient accuracy and detail over an entire catchment (Bárdossy, 2007). These parameters are generally calibrated against observed time series values, for example, river discharge data, in order to identify a suitable parameter set which enables the model to match observed discharge. However, due to lack of observed datasets to compare, the models are difficult to apply directly in the ungauged catchment. The application of rainfall–runoff models is particularly challenging in the Himalayan region, where meteorological stations are sparse, with few at high altitude and the majority located in river valleys where precipitation is often lower; discharge measurements are limited; and the quality of measured data is generally low (Immerzeel, Wanders, Lutz, Shea, & Bierkens, 2015; Nepal et al., 2014).

A number of methods have been proposed for understanding the hydrology of ungauged catchments. Rees, Holmes, Young, and Kansakar (2004) proposed recession-based hydrological models to estimate dry season flow in ungauged catchments on the basis of the recession curve behaviour. Ergen and Kentel (2015) discussed map correlation and multiple-source sites drainage-area ratio methods for estimating streamflow in ungauged basins, and Tasker (1987) reviewed different regression approaches. Blöschl (2005) and Shrestha et al. (2007) suggested transposing hydrological model calibration parameters from gauged to ungauged catchments, a process generally referred to as regionalization (Blöschl & Sivapalan, 1995). To do this, model parameters are estimated for a (gauged) donor catchment using manual or automatic calibration and the parameters are then transferred to the ungauged catchment. However, the parameters may differ in different catchments due to physical and hydrological differences (Blöschl, 2005), and the extent to which the transfer is viable in different situations needs to be investigated.

A number of authors have considered the issue of transferability of parameters between basins. Patil and Stieglitz (2014) looked at a range of parameters controlling a simple rainfall–runoff model and concluded that streamflow predictability in ungauged catchments using rainfall–runoff models was largely dependent on the transfer of a small subset of the parameters. Hydrological processes (such as runoff components and evapotranspiration) are controlled by the physiographic properties of a catchment (Dunne, 1983). Catchments that are close to each other tend to show physical similarity and are likely to have a similar climate (the spatial proximity concept); thus, the rainfall–runoff relationship is likely to vary smoothly in space, and neighbouring catchments are assumed to behave in a hydrologically similar manner with similar rainfall–runoff processes. Rosero et al. (2010) suggested that a priori assignment of parameter values in parameter transferability depends on physical characteristics (such as soil and vegetation types) of catchments and the transferability of particular parameters in relation to the similarity of the characteristics of the catchments influenced by those similar parameters (such as vegetation related parameters for catchments with similar land use cover). Blöschl (2005) and Bárdossy (2007) suggested that catchments that are hydrologically similar will have similar behaviour and can be modelled using similar model parameters (Merz & Blöschl, 2004; Patil & Stieglitz, 2014). Heuvelmans, Muys, and Feyen (2004) showed that model performance declines when parameters are transferred to a catchment further away from the donor catchments. However, Rosero et al. (2010) cautioned that transfer of parameters based solely on similarity of vegetation type and soil texture is not a viable option for a priori parameter estimation; rather, interaction between these parameters is important.

In this study, we investigate the transferability of model parameters from one glaciated alpine catchment to a physically similar nearby catchment in the Eastern Himalayas using the process-based J2000 hydrological model. This model calculates the water balance in daily time steps and the underlying hydrological processes on the basis of distributed modelling entities (hydrological response units or HRUs). The processes are controlled by calibration parameters, whereas the spatial properties are retained at HRU level in the form of distributed parameters for soil, land use, topography, and geology. Thus, the J2000 hydrological model can retain the spatial variability of static landscape features. The model was applied in the donor catchment, and the validated model parameters were then transferred to the neighbouring catchment. Sensitivity and uncertainty analyses were carried out to investigate the variation in sensitivity of the parameters in both catchments. Testing the transferability of parameters basically means using the proxy-basin test (Klemeš, 1986) to determine the portability of the calibrated model and its parameter set for regional application in other gauged and ungauged river basins for applications related to sustainable water resources development. The performance of the model in the two catchments is compared and the results are discussed. Furthermore, we compare not only the simulated

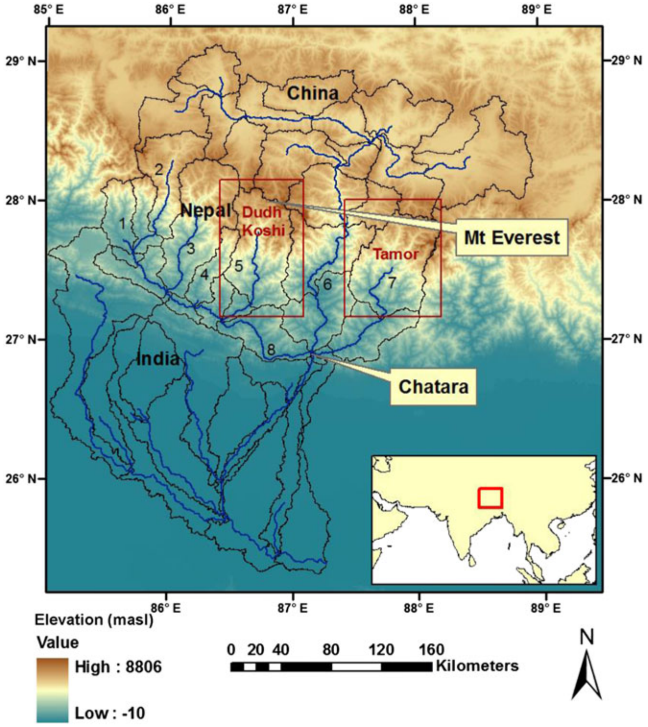

FIGURE 1 The Koshi river basin and its subcatchments (1: Indrawati, 2: Bhote Koshi, 3: Tama Koshi, 4: Likhu Khola, 5: Dudh Koshi, 6: Arun, 7: Tamor, and 8: Sun Koshi)

hydrographs but also the behaviour of the parameter sensitivity and uncertainty in both basins.

2 | MATERIALS AND METHODS

2.1 | Study area

The study was carried out in two subcatchments of the Koshi (or Kosi) river basin in the Central Himalayas (Figure 1). The Koshi river is a major tributary of the Ganges; it has an area of approximately 87,460 km^2—about 23% (19,685 km^2) in the Ganges Plains in India, 45% (39,407 km^2) in the Himalayas in Nepal, and 32% (28,368 km^2) in the lee of the Himalayan ridge on the Tibetan Plateau in China. The basin has a very large elevation range from the peak of Mt. Everest, the highest point in the world, to the low-lying plains. The Koshi river has seven major tributaries, most of which originate in high-altitude areas characterised by glaciers and permafrost (Figure 1). The tributaries meet at Chatara to form the Sapta Koshi (literally seven rivers), which flows down to the alluvial plains of Nepal and Bihar in India. The discharge and sediment load from the upstream catchments during the summer monsoon contribute to annual floods and river bank erosion, which have a marked impact on the livelihoods of the rural population, giving the river a further name of the "Sorrow of Bihar."

The Dudh Koshi and Tamor subcatchments were selected for the modelling study to test the portability of model parameters. These two catchments are part of the larger Koshi River basin. Located in a similar climatic zone, with hydrometeorological stations mostly dominated in low-altitude areas and comparable basin size, these subcatchments promised a good potential to test the parameter transferability concept. The comparison of the catchment properties are provided in the next section. Figure 2 shows the physiographic landscape type, elevation range, climate zone, and land cover across the Koshi basin, including in the two subcatchments. The geological strata, soil types, and land use and land cover are controlled by physiographic landscape and climate zones as shown in Figure 2 and can be considered similar for two subcatchments being located in a neighbouring catchment. The hydrometeorological stations in the two catchments are shown in Figure 3 (upper panel); the low level of monitoring infrastructure is clearly evident, especially at higher elevation.

2.2 | Comparison of catchment properties

The physiographic landscape, land use and land cover, and climate characteristics of the two subcatchments are illustrated in Figure 2 and summarised in Table 1. These are compared to learn the similarities in static landscape features that develop a basis to transfer the J2000 model parameters.

1. Both subcatchments are characterised by steep topography in the Lesser Himalaya and high mountains in the Higher Himalaya.
2. The land use and land cover pattern is closely linked to the distribution of the elevation bands and influenced by the monsoon climate. The subtropical lower middle mountain elevation range of the Lesser Himalaya is dominated by deciduous forest, whereas the upper elevation of the higher Himalaya is covered by coniferous forest and alpine grassland, giving way to bare rock, glaciers, and snow in the highest areas.
3. The soil properties in the subcatchments are also related to the elevation zones (Figure 3, middle panel). The Lesser Himalaya region is dominated by a pattern of Cambisols, Umbrisols, and Regosols characterised by medium to fine textured loamy to fine loamy soils. The Higher Himalayas are dominated by Regosols, which are little developed mineral soils with unconsolidated and

FIGURE 2 Physiographic landscapes, climate zones, and associated land cover of the Koshi river basin in Nepal and China. The Dudh Koshi and Tamor subcatchments extend from the Lesser Himalaya to the Higher Himalaya on the southern slopes of the range. (Source: modified from Regmee, 2004), Note: MFT = main frontal thrust; MBT = main boundary thrust; MCT = main central thrust

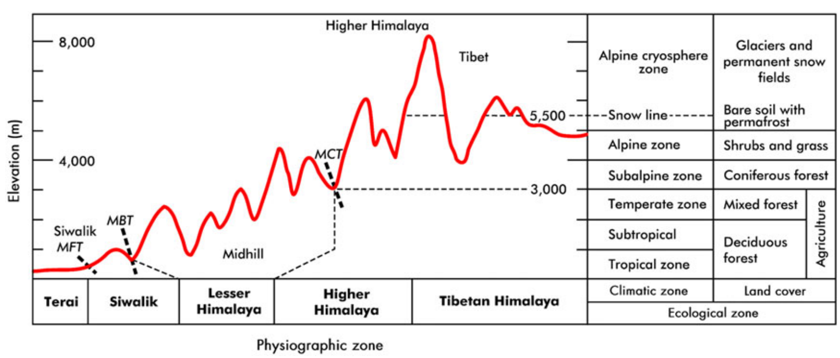

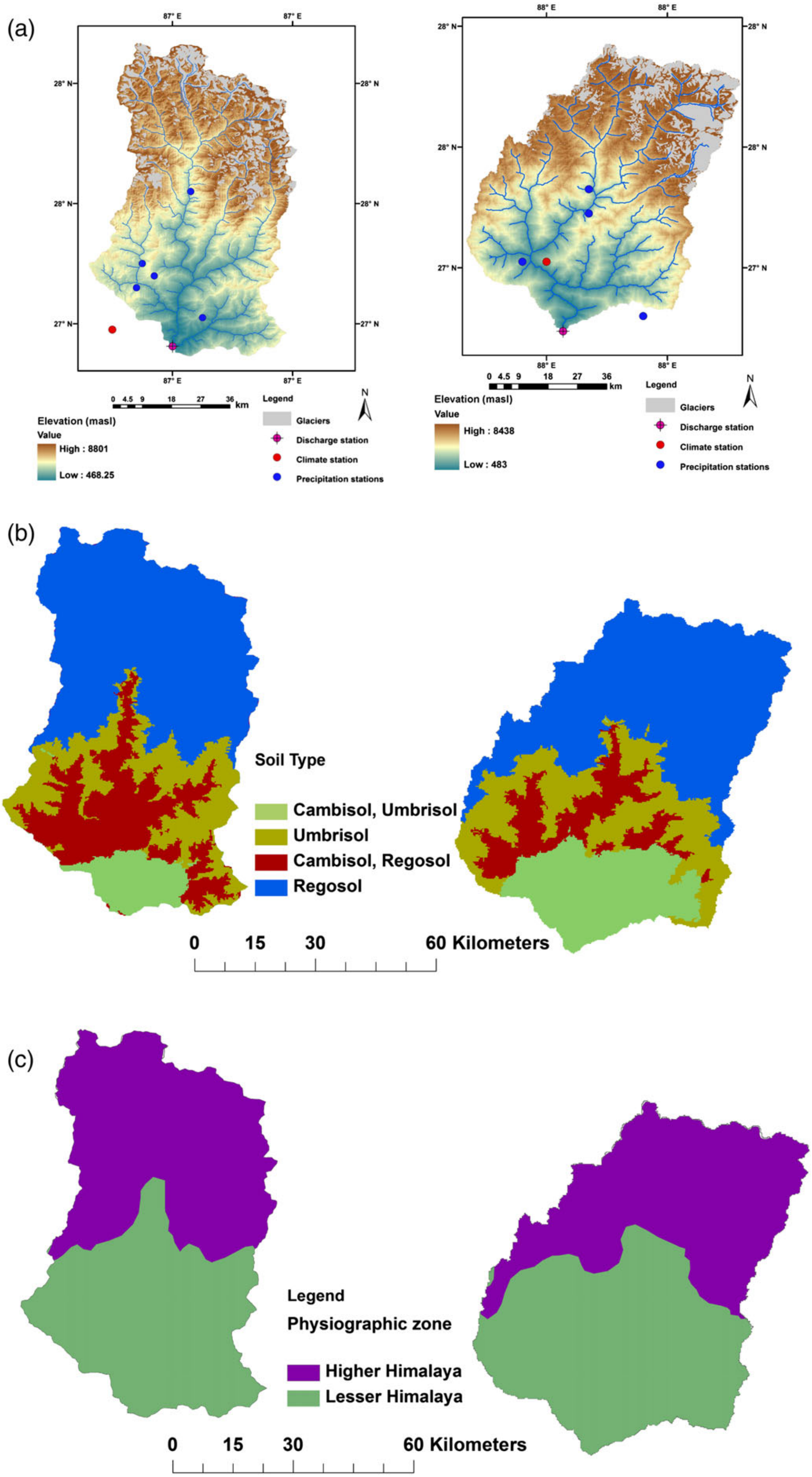

FIGURE 3 The Dudh Koshi (left) and Tamor (right) subcatchments showing the river networks and hydrometeorological stations (upper panel), soil types (middle panel) and physiographic division which provides the basis for the geological parameters (lower panel)

TABLE 1 Characteristics of the Dudh Koshi and Tamor subcatchments

Characteristics	Dudh Koshi	Tamor
Area (km^2)	3,712	4,005
Elevation (masl)		
Maximum	8,048	8,398
Average	3,590	3,403
Minimum	502	516
Average slope (degrees)	27	27
Land cover (%). Data source: GlobCover (Defourny et al., 2006)		
Forest	41	48
Grassland	4	6
Shrubland	3	4
Agriculture	11	9
Bare land	25	18
Rock/water bodies	2	1
Glacier	14	13
Glaciated area below 5,500 masl[a] (%) (km^2)	60 (301)	32 (171)
Soil (%). Data source (SOTER database)		
Regosol (HH)	43	47
Cambisol/Umbrisol (LH)	7	19
Umbrisol (LH)	26	22
Cambisol/Regosol (LH)	24	12
Geology		
Higher Himalaya	Strongly metamorphosed rock, groundwater storage capacity less than in the Lesser Himalaya	Strongly metamorphosed rock, groundwater storage capacity less than in the Lesser Himalaya
	Area (62%)	Area (59%)
Lesser Himalaya	Sedimentary, and metasedimentary rocks, storage capacity higher than in the higher Himalaya	Sedimentary, and metasedimentary rocks, storage capacity higher than in the higher Himalaya
	Area (38%)	Area (41%)
Precipitation	1985–1997	2001–2009
Annual average (mm)	1,934	2,124
Summer monsoon (%)	82	73
Discharge		
Total annual mean (mm)	1,602	1,734
Rainfall–runoff coefficient based on the observed data (%)	83	82

[a]Average equilibrium-line altitude (ELA) taken to be 5,500 masl; range 5,355–5,800 masl

coarse textured materials. The relative percentage of the different soil types is similar in the two subcatchments (Table 1).

4. Topography is the major factor controlling the pattern of rainfall and runoff generation, with different patterns in the Lesser and Higher Himalaya (Dahal & Hasegawa, 2008). These zones were used to derive the hydrogeological parameters for the subcatchments (Figure 3, lower panel) to represent groundwater storage, whereas the glaciated high-altitude areas were considered to be a single geological type with no infiltration and no soil or groundwater storage (Table 1). The area of land within the different geological zones was similar in the two subcatchments.
5. The distribution of overall area, and of glaciated area, in the different elevation bands in the two subcatchments is shown in Figure 4. The overall distribution is similar between 3,000 and 5,000 masl, but there are some differences in the area of land below 3,000 masl (greater area in the Tamor) and above 5,000 masl (greater area in the Dudh Koshi). The majority of the glacier areas lies between 5,000 and 6,000 masl in both subcatchments, but the proportion above and below the average equilibrium-line altitude (ELA) of about 5,500 masl. The ELA value was taken from the Dudh Koshi subcatchment and calculated as an average of the range of 5,335 to 5,800 masl as suggested by Wagnon et al. (2013). This elevation band is expected to be sensitive to melt runoff (Shea, Immerzeel, Wagnon, Vincent, & Bajracharya, 2015).

Overall, the comparison of catchment properties indicates a high degree of similarity between the two subcatchments in terms of

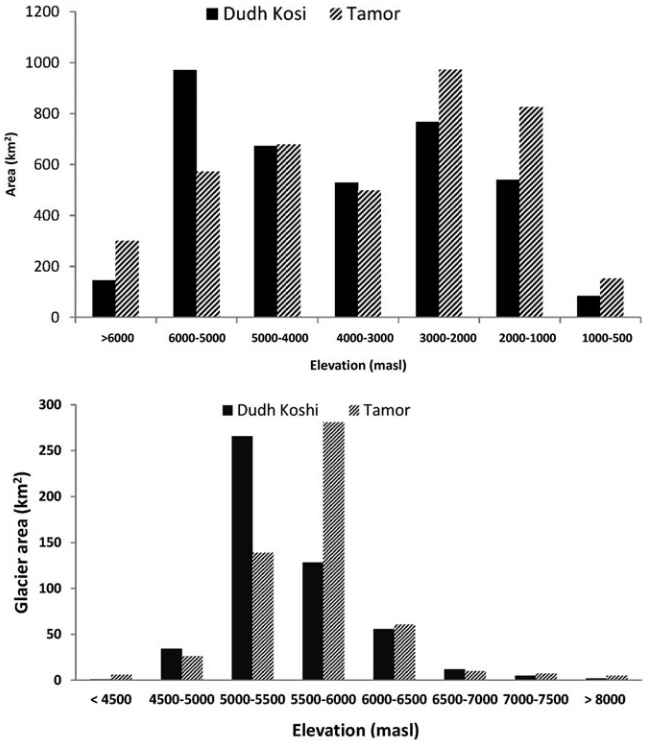

FIGURE 4 The distribution of land (top) and glacier (bottom) area in different elevation zones in the two subcatchments

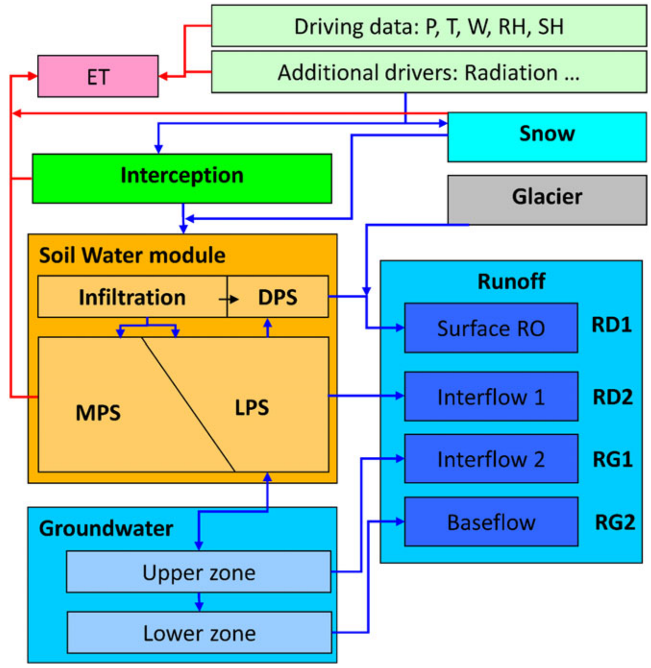

FIGURE 5 The principal layout of the JAMS/J2000 hydrological model (adapted from Krause, 2001 and Nepal et al., 2014). Note: P = precipitation; T = air temperature; WS = wind speed; RH = relative humidity; SH = sunshine hour; LPS = large pore storage; MPS = middle pore storage; DPS = depression storage; RO = runoff

topography, physiographic zones and precipitation and discharge patterns which was the reason for choosing Dudh Koshi and Tamor as the test catchments for this study.

2.3 | The J2000 model

The J2000 is a process-oriented hydrological model for the simulation of river basin water balance components and river discharge at mesoscale and macroscale basins. The model has a modular structure and is implemented in the Jena Adaptable Modelling System (JAMS), which is a model framework system for component-based development and application of environmental models (Kralisch & Krause, 2006; Kralisch et al., 2007). A short description of the model is provided below; a more detailed description of the model structure and its modules is given in Krause (2001, 2002) and Nepal (2012).

The J2000 model has a process description incorporating important hydrological processes such as precipitation distribution, interception, snow, glacier, soil moisture, groundwater, and flow routing. The principal layout is shown in Figure 5. The model produces four runoff components representing river discharge, that is, overland flow (RD1), interflow 1 (RD2), Interflow 2 (RG1) and baseflow (RG2) as shown in Figure 5 and described in Nepal (2012). The JAMS modelling framework and J2000 model are open access including source code and can be downloaded from http://jams.uni-jena.de.

2.4 | Model input data and modules within J2000

The model requires precipitation, temperature, relative humidity, sunshine hour, and wind speed as daily input data to calculate different hydrological processes. For catchment distribution, the precipitation is regionalized from precipitation stations to the HRU by applying inverse distance weighting (IDW). Similarly, the temperature is interpolated by using summer and winter seasonal lapse rates, respectively. The lapse rates were calculated from two climate stations in the Dudh Koshi subcatchment with a short period of data (Nepal, 2012). Precipitation is divided into rain and snow depending upon the air temperature. The potential evapotranspiration (PET) is calculated using the FAO Penman–Monteith approach (Allen, Pereira, Raes, & Smith, 1998) and is then checked against the actual water storage in different landscape compartments (such as interception, snow, and soil water) to determine the actual evapotranspiration (AET).

The "interception module" estimates the amount of precipitation intercepted at the vegetation cover of the HRU. The "snow module" processes the snow part of the precipitation and considers depth, density, and the content of liquid and frozen water of the snow. The model considers the energy input from air temperature, precipitation, and soil temperature in the form of calibration parameters. The potential snow melt is considered as liquid water and is stored in the pore system of the snowpack until a critical snow density is reached. The storage capacity of the snowpack is almost completely lost when a certain amount of liquid water in relation to the total snow water equivalent (SWE) is reached (Bertle, 1966). In the model, the snowmelt runoff from the snowpack is then released and passed to the soil module. The "glacier module" simulates ice melting in the glacier HRU and applies an enhanced degree day factor as proposed by Hock (1999). First, the seasonal snow falls on the glacier surface and melts as described in the snow module. When snow storage is zero on the glacier area, the ice melting process starts. Glacier ice melt on debris-covered glaciers is reduced by a debris-cover factor, which is controlled by the calibration parameter. Ice and snowmelt together with rain runoff (rain-on-snow on glacier surface) are then routed through the glaciated areas and supplied to the nearby stream. The "soil module" represents the processes in the unsaturated part of the soil with two storage types: the middle pore storage (MPS) and the large pore storage (LPS). The soil moisture conditions influence the infiltration process; thus, the infiltration capacity is calculated on the basis of the actual soil moisture. The water stored in the MPS is considered as field capacity and reduced by potential evapotranspiration. The water in the LPS is distributed between the lateral and vertical water flow components. The lateral flow is responsible for producing interflow from the unsaturated zone (RD2). The "groundwater module" handles the groundwater storage for each HRU and receives the vertical flow percolating through the soil. The water discharge from the upper and lower storage areas (RG1 and RG2) is modelled in relation to the actual storage by means of a linear function, using the storage retention coefficient for two storages (Krause et al., 2006). The runoff components generated through each HRU are routed to the next connected HRU until a model entity is connected to the river network. Inside the river network, the "channel routing" is considered using a simplified kinematic wave approach and the calculation of flow velocity according to Manning–Strickler as described in Krause (2001).

2.5 | Model parameters

The hydrological modules contain a number of calibration parameters for adaptation of the model response. Table 2 shows 36 calibration parameters that were optimised to improve the fit between observed and simulated discharge (see calibration procedure below). In addition to the calibration parameters, the J2000 hydrological model has separate parameter files that represent the spatial and temporal heterogeneity of the basin landscape (slope, elevation, and aspect), vegetation (e.g. leaf area index and rooting depth), soil (field capacity and LPS), and geology (water storage capacity of aquifers and retention period). These are compiled in the HRU parameter file (and connected to the respective parameter files) in which the hydrological processes are controlled by calibration parameters.

2.6 | Distribution concept

The watershed is distributed in the model by using the concept of hydrological response units (HRUs) (Flügel, 1995). The HRUs are spatial modelling entities with a common land use, soil, geology and topography, controlling their hydrological dynamics. For the two subcatchments, the DEM, soil, land use and land cover, and geology (250-m resolution) were used for HRU delineation using a method suggested by Pfennig et al. (2009) and the combination of these layers resulted in 3,799 HRUs for the Dudh Koshi subcatchment and 3,445 HRUs for the Tamor subcatchment. Each of the hydrological processes described above for the different modules (see Figure 5) is calculated for each time step in each HRU.

2.7 | Model calibration, validation, sensitivity, and uncertainty analysis

The model was calibrated (years 1986–1991, with 1985 for model initialization) in the Dudh Koshi subcatchment using a combination of manual (trial-and-error) and automatic (Monte Carlo simulations) approaches and validated for the period of 1992–1997. Details are provided in Nepal et al. (2014). Sixteen parameters (Tables 2 and 3) were selected as they were found to be influential based on experience from a trial-and-error approach and a previous study by Bäse (2005) to use in the sensitivity and uncertainty analyses (SUA). The sensitivity analysis helps understand the nature of the model parameters in terms of their influence on the total model outputs, with sensitivity defined as the effect of the parameters on the overall model performance as indicated by the objective functions, in this case, Nash–Sutcliffe (ENS) and log Nash–Sutcliffe (LNS) (McCuen, 2005). Altogether 1,600 simulations were carried out representing 100 simulations per parameter. A uniform random sampling method was used in which the value of the parameter for each simulation was chosen within a range provided. The OPTAS toolbox implemented in the JAMS framework was used for the SUA (Fischer, Kralisch, Krause, & Flügel, 2012). A regional sensitivity analysis (RSA) was used to analyse the sensitivity of the model parameters as suggested by Hornberger and Spear (1981) and was further instrumental in obtaining a subset from the larger set of parameters for model optimization. In this way, the most optimal parameter values, as shown in Table 2, were identified and then used for the validation period. A generalized likelihood uncertainty analysis (GLUE) was used for parameter uncertainty estimation (Beven & Binley, 1992). The GLUE method is a procedure for uncertainty assessment on the basis of Monte Carlo simulations and accounts for all sources of uncertainty, that is, input data, parameters, and model structure. In this study, GLUE was used for parameter uncertainty only as other sources of uncertainty (input data and model structure) are beyond the scope of this study. Because of the lack of stations in high-altitude areas, uncertainty from input data might be similar in both subcatchments. The ensemble of 1,600 simulations from the given parameter range as shown in Table 3 was plotted against the observed hydrograph to check if the observed values were within the ensemble range.

The model parameters calibrated and validated for the Dudh Koshi subcatchment were then transferred to the nearby Tamor subcatchment for the years 2001–2009 (Year 2000 as model initialization). Although the model run period for the Tamor subcatchment is different than the Dudh Koshi, the parameter transferability actually represents the climate input dataset that was different from the donor catchment's periods. In this way, the transferability of parameters represent both spatial and temporal dimensions. The model results from both subcatchments in terms of simulated hydrograph were discussed. The sensitivity and uncertainty analyses were carried out in both subcatchments using similar parameter ranges (Table 3). In terms of parameter transferability, a systematic sensitivity and uncertainty analyses in both subcatchments suggest similarity and dissimilarity of hydrological processes in reference to calibration parameters. If sensitivity rank of the parameters matched well for both catchments, it can be interpreted that the catchments are dominated by similar hydrological processes that are represented through the calibration parameters.

The efficiency of the model was evaluated against three objective functions—ENS, LNS, and the coefficient of determination (r^2)—using the observed discharge data from the two gauging stations. The ENS represents the overall hydrograph with a focus on high flow

TABLE 2 Calibration parameters in the J2000 hydrological model

Parameter	Description	Value	Normal range	Dimension
Precipitation distribution				
Trs	base temperature	0	−1 to +1	°C
Trans	parameter range for mixed rain and snow	2	−2 to +2	°C
Interception module				
a_rain	interception storage for rain	1.00	0–5	mm
a_snow	interception storage for snow	1.28	0–5	mm
Snow module				
snowCritDens	critical density of snow	0.381	0–1	%
snowColdContent	cold content of snow pack	0.0012	0–1	NA
snowBaseTemp	**threshold temperature for snowmelt**	0	−5 to +5	°C
snowTfactor	**melt factor by sensible heat**	2.84	0–5	NA
snowRfactor	melt factor by liquid precipitation	0.21	0–5	NA
snowGfactor	melt factor by soil heat flow	3.73	0–5	NA
Glacier module				
meltFactorIce	**melt factor for ice melt**	2.5	0–5	NA
alphaIce	radiation melt factor for ice	0.2	0–5	NA
kIce	routing coefficient for ice melt	10	0–50	NA
kSnow	routing coefficient for snowmelt	5	0–50	NA
kRain	routing coefficient for rainfall–runoff	5	0–50	NA
debrisFactor	debris factor for ice melt	3	0–10	NA
glacierTbase	**threshold temperature for snowmelt**	−1	−5 to +5	°C
Soil module				
soilMaxDPS	maximum depression storage	2	0–10	mm
soilLinRed	**linear reduction coefficient for AET**	0.6	0–1	
soilMaxInfSummer	**maximum infiltration in summer**	60	0–200	mm
soilMaxInfWinter	**maximum infiltration in winter**	75	0–200	mm
soilMaxInfSnow	maximum infiltration in snow cover areas	40	0–200	mm
soilInpLT80	infiltration for areas less than 80% sealing	0.5	0–1	NA
SoilDistMPSLPS	MPS-LPS distribution coefficient	0.27	0–10	NA
SoilDiffMPSLPS	MPS-LPS diffusion coefficient	0.1	0–10	NA
soilOutLPS	outflow coefficient for LPS	0.3	0–10	NA
soilLatVertLPS	**lateral vertical distribution coefficient**	0.5	0–10	
soilMaxPerc	**maximum percolation rate to groundwater**	10	0–100	mm
soilConcRD1Flood	**recession coefficient for flood event**	1.3	1–10	NA
soilConcRD1Floodthreshold	threshold value for soilConcRD1Flood	300	0–500	NA
soilConcRD1	**recession coefficient for overland flow**	2.8	1–10	NA
SoilConcRD2	**recession coefficient for interflow**	3	1–10	NA
Groundwater module				
gwRG1RG2dist	**RG1-RG2 distribution coefficient**	2.1	0–5	NA
gwRG1Fact	**adaptation factor for RG1 flow**	0.3	0–10	NA
gwRG2Fact	**adaptation factor for RG2 flow**	0.5	0–10	NA
gwCapRise	capillary rise coefficient	0.01	0–10	NA
Reach routing				
flowRouteTA	**flood routing coefficient**	1.3	0–10	NA

Note. Bold = sensitive parameters.

TABLE 3 Parameter ranges for sensitivity and uncertainty analyses

Selected parameters	Parameter range	
	Low	High
snowBaseTemp	−3	3
snowTfactor	0.5	5
glacierTbase	−3	3
glacierMeltFactorIce	0.5	5
flowRouteTA	0.1	5
gwRG1Fact	0.01	3
gwRG1RG2dist	0.5	4
gwRG2Fact	0.01	3
soilConcRD1	1	5
soilConcRD1flood	1	3
soilConcRD2	1	5
soilLatVertLPS	0.1	3
soilLinRed	0.5	2.5
soilMaxInfSummer	30	100
soilMaxInfWinter	30	120
soilMaxPerc	5	15

conditions. The ENS is sensitive to high flow conditions. The LNS was calculated with logarithm observed and predicted values. LNS flattens the runoff, and high flows and low flows are kept more or less at the same level (Krause, Boyle, & Bäse, 2005). The r^2 provides the variability of the observed and measured stream flows.

3 | RESULTS AND DISCUSSION

3.1 | Hydrological modelling

The Dudh Koshi subcatchment has six precipitation stations, one of them also a climate station (temperature, relative humidity, wind speed, and sunshine hours), and the Tamor has five precipitation stations, one providing climate data as well (Figure 3 and Table 4). Data from the earlier period, compared to Tamor subcatchment, were used for the Dudh Koshi as a glacial lake outburst flood (GLOF) event in the catchment in September 1998 (Osti & Egashira, 2009) severely damaged the Rabuwabazaar gauging station and affected the quality of the discharge data afterwards (Nepal, 2012).

The precipitation dynamics in both subcatchments is dominated by the Indian summer monsoon system; most of the precipitation occurs during the summer season between June and September (Nepal, 2012). The average annual precipitation is about 10% higher in the Tamor subcatchment as shown in Table 4. The annual average discharge from the Dudh Koshi (1,602 mm) was slightly lower than from the Tamor (1,734 mm). However, the rainfall–runoff coefficient, which represents how much rainfall is converted to runoff, suggests a similar value (Table 1).

Figure 6a shows the simulated and observed discharge from the Dudh Koshi subcatchment during the validation period (Nepal et al., 2014). The model simulated the base flow quite well in most events. The recession periods are also well captured although a slight underestimation can be observed in some years. The rising limbs are also represented reasonably well, although there is some overestimation during the pre-monsoon period in 1992 and 1994. The model represented flood periods fairly well, although with a slight underestimation in 1993 and over prediction in 1994. The 1996 and 1997 flood events are captured well, although slight underestimation in 1997. For a closer look, a representative hydrograph for the year 1995 (NSE: 0.86) is provided in Figure 6b. Similar results were observed during the calibration period (Nepal et al., 2014). Overall, the J2000 model is able to represent different parts of the hydrograph both for calibration and validation periods. However, the underestimation and overestimation in different years can be attributed to different reasons: lack of representative data in high-altitude areas, limitation of rating curves to estimate discharge data (especially during the monsoon season), and model structure and related parameters to represent various hydrological processes. Table 5 shows the model efficiency results for the Dudh Koshi subcatchment for the entire period. On the basis of the performance rating for the recommended statistics suggested by Moriasi et al. (2007), "very good" results were obtained for ENS, LNS, and the r^2, with slightly better results in the validation period.

3.2 | Transfer of model parameters to the Tamor subcatchment

The Dudh Koshi and Tamor subcatchments have a high degree of similarity in terms of their static landscape features (Table 1). Using the proxy-basin approach, the parameters from the calibrated and validated Dudh Koshi model were transferred to the Tamor subcatchment and the model was evaluated for the period 2001–2009. Figure 7a shows the observed and simulated stream flows. The model represented the base flow, rising limbs, and recession periods quite well in most years, but peak events were generally underestimated. The highest flood peak event is captured well during 2005 whereas the events are underestimated for 2001–2003 and 2007–2009. For a closer look, a representative hydrograph for the year 2005 (NSE: 0.81) is provided in Figure 7b. Overall, the transferred parameters produced the discharge conditions during the dry season, but with underestimation of flood peaks in a number of years.

The efficiency results for the model evaluation with different objective functions are shown in Table 5. The efficiency values were generally good and slightly better for low flow conditions as indicated by the higher values against LNS. The model efficiency results were similar to those observed for the nearby Dudh Koshi subcatchment where the model was calibrated and validated.

Although, a good efficiency result is achieved with transferred parameter to Tamor subcatchment for different periods than the Dudh Koshi subcatchment, underestimation of peaks could be due to many reasons ranging from simple conceptualization of model for flood processes, underestimation of rainfall due to the lack of high-altitude stations, and transferred parameters from neighbouring catchment, nonlinearity of catchment especially during the saturated conditions. Besides, the development of discharge rating curves comprises uncertainty especially during the high flow season. As discussed by Nepal (2012) with reference to the Dudh Koshi subcatchment, the maximum water level (stage) considered for discharge estimation for the rating curve for flood season is below 710 m^3/s. In the case of Tamor, the maximum water level considered

TABLE 4 Location, elevation, and annual mean precipitation of the hydrometeorological stations in the Dudh Koshi and Tamor subcatchments

Station		Latitude (deg)	Longitude (deg)	Elevation (masl)	Annual mean precipitation (mm)	Annual mean discharge (mm)	Subcatchments map with station IDs
Dudh Koshi							
ID	Name				(1985–1997)		
670	Rabuwabazaar (D)	27.26	86.65	670		1,602	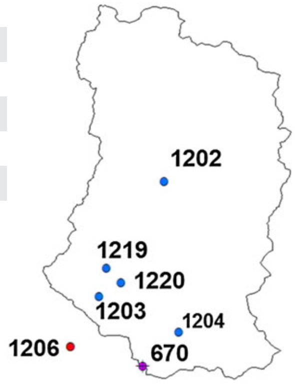
1202	Chaurikark (P)	27.42	86.43	2,660	2,096		
1203	Pakarnas (P)	27.26	86.34	1,982	1,885		
1204	Aiselukhark (P)	27.21	86.45	2,143	2,417		
1206	Okhaldhunga (C)	27.19	27.19	1,720	1,805		
1219	Sallery (P)	27.3	86.35	2,378	1,592		
1220	Chialsa (P)	27.46	86.61	2,770	1,806		
Tamor							
					(2001–2009)		
684	Majhitar[a] (D)	27.15	87.71	684		1,734	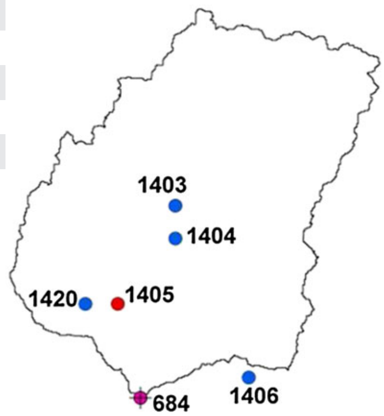
1403	Lungthung (P)	27.33	87.47	1,780	2,339		
1404	Taplethok (P)	27.29	87.47	1,383	2,397		
1405	Taplejung (C)	27.21	87.4	1,732	1,946		
1406	Memenjagat (P)	27.12	87.56	1,830	2,258		
1420	Dovan[b] (P)	27.21	87.36	763	1,681		

Note. Stations: C = climate; D = discharge; P = precipitation.

[a]Data gaps in 2006 (October to December) and 2008 (March) filled by regression analysis as gaps were in the dry season when flow is low and changes consistent; in the modelling exercise, the gaps were left empty.

[b]Data gaps in 2008/2009, excluded from the analysis.

for rating curve is below 702 m^3/s. Per personal communication with Mr. Rajendra Sharma, Senior Divisional Hydrologist of the Department of Hydrology and Meteorology, Nepal, the discharge is rarely measured during rainy periods in Nepal due to the high velocity of water current during the monsoon season. The other possible reasons in reference to parameters are discussed below with reference to sensitivity and uncertainty analyses.

The results indicate that the model represented the observed stream flow in the Tamor river reasonably well using the parameters from the Dudh Koshi subcatchment. The scatter plot between observed and simulated daily discharge for the Tamor river (Figure 8) also indicates a good representation (r^2: 0.84), with relatively good agreement below 500 m^3/s, but some differences can be seen during high flows (for the scatter plot of the Dudh Koshi [r^2: 0.86], please refer to Nepal et al. (2014). The simulated discharge is underestimated by 8% in the Tamor subcatchment compared to 1% in the Dudh Koshi.

Amongst other things, the transferred parameters were directly used without any further adjustment. The results might be improved if the parameters are further adjusted (e.g., a slight increase in *FloodRoutingTA* also increases NSE slightly in Tamor). However, within the limitation of this study, our main aim was to show that the transferred parameters also work well provided the neighbouring basins have physical similarity.

3.3 | Sensitivity and uncertainty analyses

Figure 9 shows the distribution of the 16 selected parameters in the two subcatchments in three parameter sensitivity zones. The weightage for each parameter is defined by the RSA from 1,600 simulations for Nash–Sutcliffe (Figure 9, top) and log Nash–Sutcliffe (Figure 9, bottom) efficiencies. If all parameters had an equal effect on the model behaviour, each would have a weightage of 0.06 (1 out of 16 parameters). Highly sensitive parameters are defined as those with a weightage > 0.18

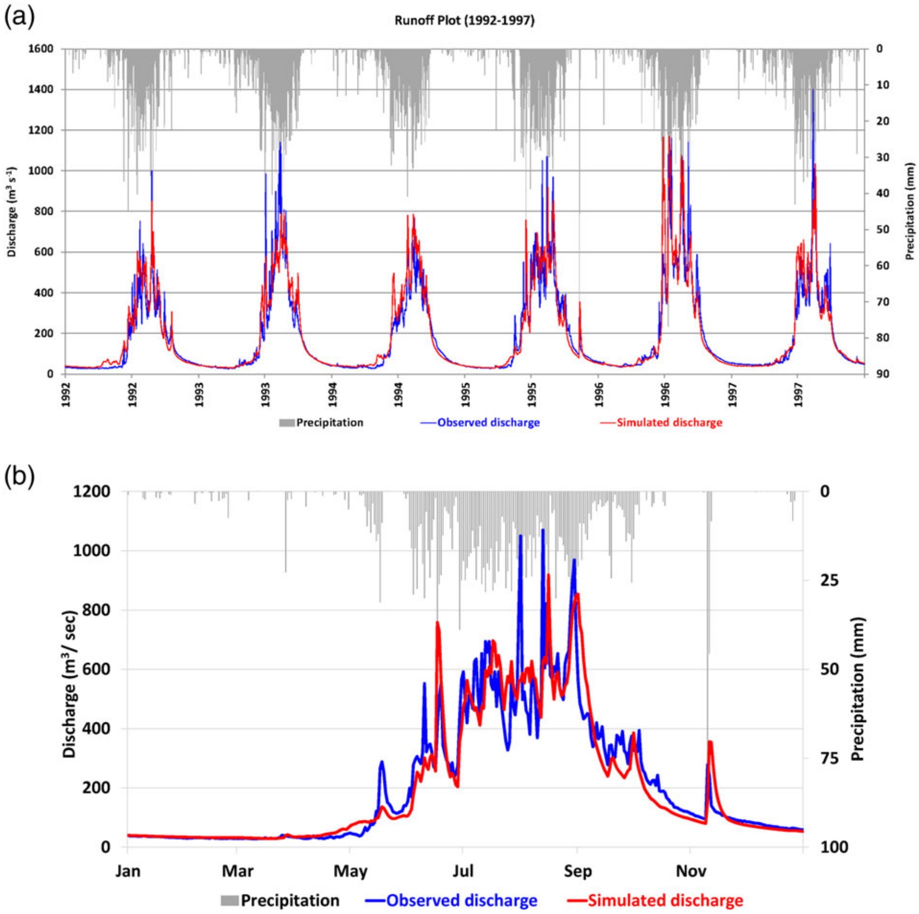

FIGURE 6 (a) The simulated and observed discharge of the Dudh Koshi subcatchment during the validation period (1992–1997); (source: Nepal et al., 2014). (b) Observed versus simulated hydrograph for the year 1995

TABLE 5 Model performance efficiency

Objective function	Dudh Koshi Calibration 1986–1991	Dudh Koshi Validation 1992–1997	Tamor
Nash–Sutcliffe (ENS)	0.84	0.87	0.84
Log Nash–Sutcliffe (LNS)	0.90	0.95	0.93
Coefficient of determination (r^2)	0.85	0.88	0.84

(equivalent of more than three parameters' weightage); moderately sensitive with a weightage of 0.06 to 0.18, and less sensitive with a weightage of <0.06. The parameter *soilLatVertLPS* was the most sensitive parameter for Nash–Sutcliffe efficiency in both subcatchments with a weightage of nearly 0.34 in Dudh Koshi and 0.29 in Tamor. This parameter distributes the excess water (after infiltration) to interflow 1 and percolation depending upon the slope of the HRU. Therefore, it has a strong influence on the composition of the modelled runoff components and the shape and the timing of the modelled hydrograph. Altogether, 13 of 16 parameters were in the same sensitivity range for Nash–Sutcliffe efficiency in both basins, whereas three parameters—*glacierTbase*, *flowTouteTA*, and *soilConcRD2*—were in different sensitivity zones. The variation in *glacierTbase* is probably due to the difference in the glacier area below 5,500 masl, the effective melting zone (301 km^2 in Dudh Koshi and 171 km^2 in Tamor). The variation in *flowRouteTA* might be due to differences in size and slope of the reaches; the total reach length is 5% higher in the Tamor, whereas the lowest slope reaches in the Dudh Koshi were 0.001% compared to 0.12% in Tamor. Moreover, the routing process in J2000 is a very simplified representation of the river routing processes, which are neglecting different profiles and runoff obstacles. Combination of these might be the reason of underestimation of flood peaks in the Tamor subcatchment compared to the Dudh Koshi. The reasons for the variation in *soilConcRD2* remain unclear; more detailed analysis of the topographic properties and experiments with variations in parameter change might help to pinpoint the cause of the difference. Some parameters were found to be sensitive over others as they can influence the large volume of water and also the hydrograph. The range of the selected parameters (Table 3) also plays a key role in setting sensitivity of parameters. Having a larger range means the model will produce nonbehavioural simulations that can influence sensitivity.

The similar pattern of the parameter sensitivity is an indication that the two subcatchments feature a similar hydrological response to rainfall. On the other hand, such patterns could be taken as an indicator as to whether a parameter transfer to an ungauged catchment might be feasible or not.

Figure 10 shows the results of the generalized likelihood uncertainty estimation (GLUE) for the two subcatchments with the ensemble of 1,600 model simulations compared with the observed

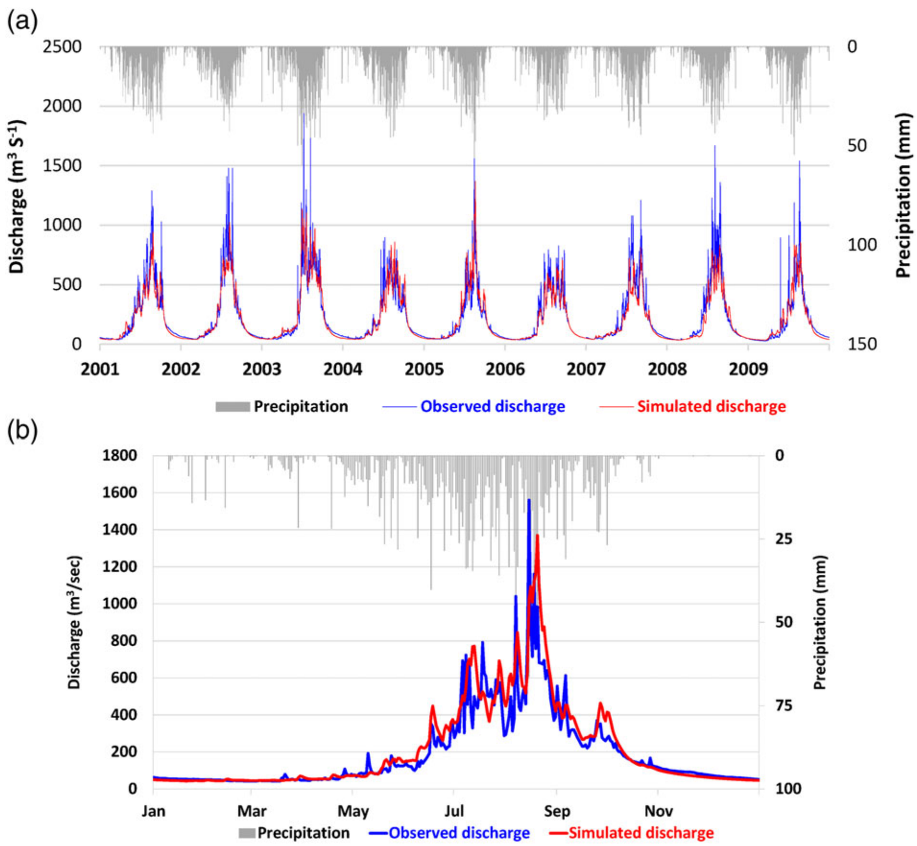

FIGURE 7 (a) The simulated and observed discharge of the Tamor subcatchment for 2001–2009. (b) Observed versus simulated hydrograph for the year 2005

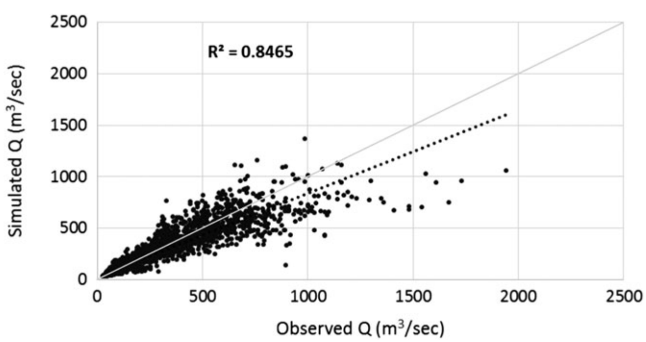

FIGURE 8 Scatter plot between observed and simulated discharge (Q) in the Tamor subcatchment

hydrograph values. The ranges chosen were narrower than the normal range for J2000 (Table 3) and were determined on the basis of trial-and-error, expert knowledge, and catchment characteristics. The results are shown for the last year used for validation in both subcatchments. As shown in the figure, most of the time the observed runoff is within the parameter uncertainty range, although occasionally the values lie outside the uncertainty range, especially during flood peaks and more events in the Tamor. This may be due to the limited input data resulting from the small number of precipitation stations and lack of representative stations in high-altitude areas, stage-discharge rating curve, and model structural uncertainty. The comparison between the modelled and simulated hydrographs (Figure 7) also showed underestimation of flood peaks for some years. This uncertainty result indicates that the parameters of the J2000 model and its representation of hydrological processes seems to be working in a similar way for neighbouring catchments. This is demonstrated in Figure 10 which shows that the observed runoff most of the time lies within the uncertainty range. Figure 11 shows the scatter plots for the ensemble mean of the 1,600 simulations with the observed discharge for the full period of model run. In both subcatchments, r^2 is 0.85, which is considered good, especially coming from the ensemble mean. The ENS values for the ensemble mean were slightly lower for the Dudh Koshi (0.76) than for the Tamor (0.81). The results suggest the possibility of using the ensemble mean for ungauged catchments instead of a single output from the modelling.

The analysis together suggest that the sensitivities of the selected parameters are mostly very similar in both subcatchments. Taken together, the results indicate that the J2000 is a viable model for parameter transfer between basins in spatial proximity and with reasonable physical similarities. This could be interpreted as (a) the two catchments have a very similar hydrological functioning, that is, the hydrological processes dominance is similar, which leads to a similar catchment response and (b) the physical basis of the J2000 model is good enough to reproduce such similar catchment response. As other studies also suggested that the catchments in physical proximity are likely to have hydrological similarity and thus can be modelled using similar parameters from donor catchments (Bárdossy, 2007; Blöschl, 2005; Merz & Blöschl, 2004).

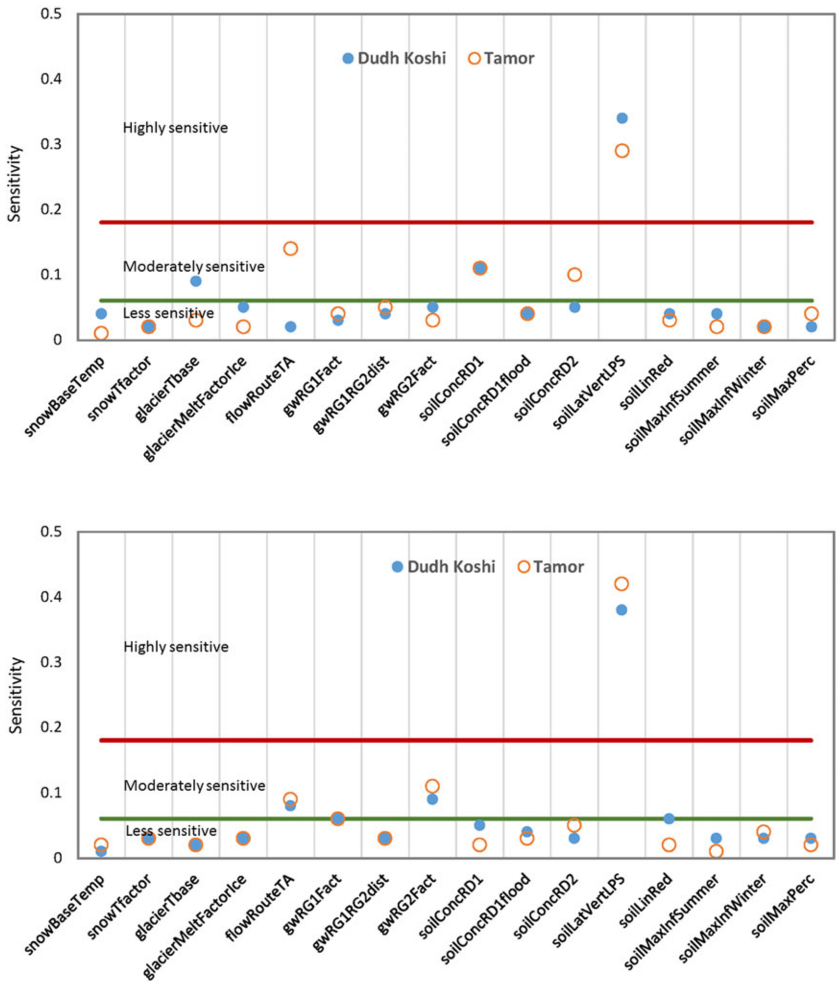

FIGURE 9 Sensitivity of parameters using regional sensitivity analysis (top: ENS; bottom: LNS)

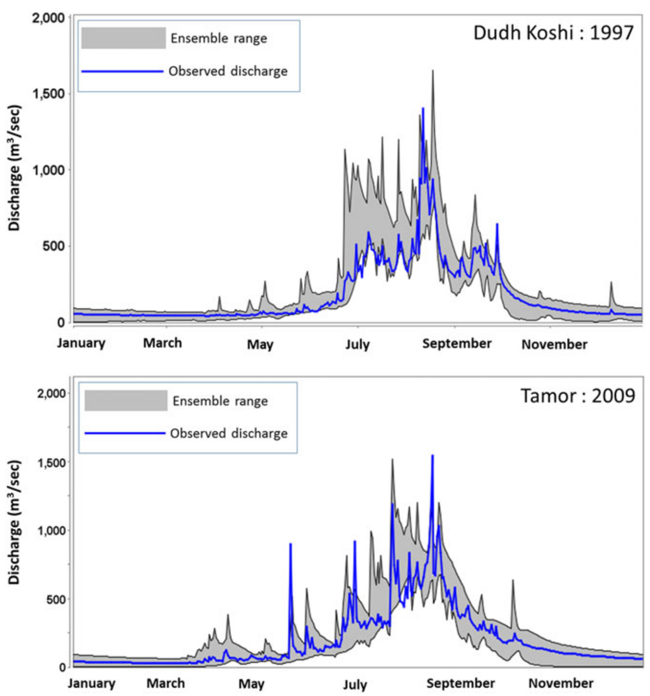

FIGURE 10 GLUE parameter uncertainty analysis in the Dudh Koshi (top) and Tamor (bottom) for the last year of the validation period

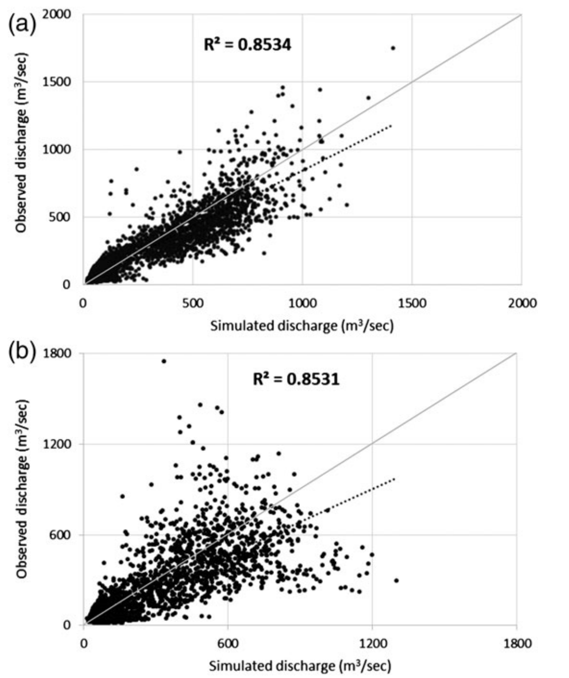

FIGURE 11 Scatter plots between ensemble mean (1,600 simulations from GLUE) and observed discharge in the Dudh Koshi (top) and Tamor (bottom) for the model run period

4 | CONCLUSIONS AND OUTLOOK

The selected subcatchments have a high degree of similarity in terms of their static landscape features and were thus suitable for investigating the viability of transferring model parameters.

The major conclusions are as follows:

1. The transferred parameters of the J2000 model represented the overall underlying hydrological process representation of the recipient catchment (i.e., Tamor) very well for the period, which was different than the donor catchment (i.e., Dudh Koshi). The proxy-basin approach was well suited as a means to test parameter transferability for the process-based J2000 model.
2. The sensitivities of the selected parameters are most of the time very similar in both catchments. The GLUE uncertainty analysis showed that the model outputs were within the range of the parameter uncertainty band; there was good agreement between the ensemble mean and observed discharge. This shows the possibility of using the ensemble mean to produce a runoff estimation in ungauged catchments. The results indicate that transfer of the J2000 model parameters to a neighbouring catchment with reasonably similar physical characteristics is viable.
3. The extent to which differences in catchment properties affect parameter variation should be explored further by applying the model and the parameter ranges listed in Table 3 to other subcatchments in the Himalayan region with differences in spatial and hydrological properties. Especially, the parameter values might differ with the scale of the basin which in turn affect the flood routing, recession coefficients, and baseflow proportions. Similarly, geological formations and land use pattern also affect the dry season flows and runoff components. Another factor that might be influential for the parameter variation is the distribution of the weather stations and their representativeness for the meteorological dynamics in the catchments. Some of the parameters in hydrological models are calibrated to cope with the coarse and incomplete representation of the meteorological dynamics in the measurement networks. This cannot be described in this analysis because in our setup show a strong similarities in both measurement networks (Figure 3). These additional analysis might provide useful insights into the hydrological system dynamics and parameterization of the J2000 model in Himalayan catchments of varying sizes and available information quality.
4. The J2000 model can be used to estimate the discharge from ungauged catchments in the Himalayan region by transferring the parameters developed for a close-by gauged catchment with similar geophysical characteristics.

ACKNOWLEDGMENTS

The study was supported by the Koshi Basin Programme at the International Centre for Integrated Mountain Development (ICIMOD), which is supported by the Australian Government through the Sustainable Development Investment Portfolio for South Asia and partly by the Federal Ministry of Education and Research (BMBF), Germany, which provided funds for a part of this study as PhD research under International Postgraduate Studies in Water Technologies (IPSWaT) programme at the Friedrich Schiller University of Jena (FSU Jena), Germany. The study was also supported in part by ICIMOD core funds contributed by the Governments of Afghanistan, Australia, Austria, Bangladesh, Bhutan, China, India, Myanmar, Nepal, Norway, Pakistan, Switzerland, and the United Kingdom. We thank the Department of Hydrology and Meteorology, Nepal for providing the hydrometeorological data required to run the model. The views and interpretations in this publication are those of the authors and are not necessarily attributable to their organisations. Finally, we are thankful to the anonymous reviewers for their constructive comments that helped to improve the manuscript significantly.

REFERENCES

Agrawala, S., Raksakulthai V., van Aalst M., Larsen P., Smith J., & Reynolds, J. (2003). Development and climate change in Nepal: Focus on water resources and hydropower. Organization for Economic Cooperation and Development, Paris 64.

Allen, R. G., Pereira, L., Raes, D., & Smith, M. (1998). *Crop evapotranspiration: Guidelines for computing crop water requirements, FAO irrigation and drainage paper 56*. FAO: Rome.

Anderson, M. G., & Burt, T. P. (1985). Modelling strategies. In M. G. Anderson, & T. P. Burt (Eds.), *Hydrological forecasting* (pp. 1–13). John Wiley & Sons: Chichester.

Bárdossy, A. (2007). Calibration of hydrological model parameters for ungauged catchments. *Hydrology and Earth System Sciences*, *11*, 703–710.

Bäse, F. (2005). Beurteilung der Parametersensitivität und der Vorhersageunsicherheit am Beispiel des hydrologischen Modells J2000. Master's Thesis, Friedrich-Schiller-Universität, Jena.

Bertle, F.A., (1966). Effects of snow compaction on runoff from rain and snow. Bureau of Reclamation, Engineering Monograph No. 35, Washington.

Beven, K. J. (2001a). How far can we go in distributed hydrological modelling? *Hydrology and Earth System Sciences*, *5*(1), 1–12.

Beven, K. (2001b). *Rainfall-runoff modelling: The primer*. Chicester: John Wiley & Sons.

Beven, K., & Binley, A. M. (1992). The future of distributed models: Model calibration and uncertainty prediction. *Hydrological Processes*, *6*, 279–298.

Blöschl, G. (2005). Rainfall-runoff modelling of ungauged catchments. In M. G. Anderson (Ed.), *Encyclopedia of Hydrological Sciences* (pp. 2061–2080). Chichester, New York: John Wiley.

Blöschl, G., & Sivapalan, M. (1995). Scale issues in hydrological modelling a review. *Hydrological Processes*, *9*, 251–290.

Bourgin, F., Andréassian, V., Perrin, C., & Oudin, L. (2015). Transferring global uncertainty estimates from gauged to ungauged catchments. *Hydrology and Earth System Sciences*, *19*(5), 2535–2546.

Dahal, R. K., & Hasegawa, S. (2008). Representative rainfall thresholds for landslides in the Nepal Himalaya. *Geomorphology*, *100*(3–4), 429–443.

DeCoursey, D. G., Shaake, J. J. C., & Seely, E. H. (1982). *Stochastic models in hydrology*(pp. 19–78). St Joseph, Michigan: American Society of Agricultural Engineers.

Defourny, P., Vancutsem, C., Bicheron, C., Brockmann, C., Nino, F., Schouten, L., & Leroy, M., (2006). GLOBCOVER: A 300 M global land cover product for 2005 using ENVISAT MERIS time series. ISPRS Commission VII Mid-term Symposium “Remote Sensing: From Pixels to Processes”, Enschede, the Netherlands, 8-11 May 2006.

Dunne, T. (1983). Relation of field studies and modeling in the prediction of storm runoff. *Journal of Hydrology*, *65*, 25–48.

Ergen, K., & Kentel, E. (2015). An integrated map correlation method and multiple-source sites drainage-area ratio method for estimating streamflows at ungauged catchments: A case study of the Western Black Sea Region. *Turkey*. *Journal of Environmental Management.*, *166*, 309–320.

Fischer, C., Kralisch, S., Krause, P., & Flügel, W.A. (2012). An integrated, fast and easily useable software toolbox allowing comparative and complementary application of various parameter sensitivity analysis methods. R. Seppelt, A.A. Voinov, S. Lange, D. Bankamp (Eds.)International Environmental Modelling and Software Society (iEMSs) 2012 International Congress on Environmental Modelling and Software. Managing Resources of a Limited Planet: Pathways and Visions under Uncertainty, Sixth Biennial Meeting, Leipzig, Germany.

Flügel, W.-A. (1995). Delineating hydrological units (HRU's) by GIS analysis for regional hydrological modelling using PRMS/MMS in the drainage basin of the River Broel, Germany. *Hydrological Processes*, *9*(3–4), 423–436.

Goswami, M., O'Connor, K. M., & Bhattarai, K. P. (2007). Development of regionalisation procedures using a multi-model approach for flow simulation in an ungauged catchment. *Journal of Hydrology*, *333*, 517–531.

Heuvelmans, G., Muys, B., & Feyen, J. (2004). Evaluation of hydrological model parameter transferability for simulating the impact of land use on catchment hydrology. *Physics and Chemistry of the Earth, Parts A/B/C*, *29*(11), 739–747.

Hock, R. (1999). A distributed temperature index ice and snowmelt model including potential direct solar radiation. *Journal of Glaciology*, *45*(149), 101–111.

Hornberger, G. M., & Spear, R. C. (1981). An approach to the preliminary analysis of environmental systems. *Journal of Environmental Management*, *12*, 7–18.

Immerzeel, W. W., Wanders, N., Lutz, A. F., Shea, J. M., & Bierkens, M. F. P. (2015). Reconciling high-altitude precipitation in the upper Indus basin with glacier mass balances and runoff. *Hydrology and Earth System Sciences*, *19*, 4673–4687.

Klemeš, V. (1986). Operational testing of hydrological simulation models. *Hydrological Sciences Journal*, *31*(1), 13–24.

Kralisch, S., & Krause, P. (2006). JAMS a framework for natural resource model development and application. In: Voinov, A., Jakeman, A., Rizzoli, A.E. (Eds.). Proceedings of the iEMSs Third Biannual Meeting "Summit on Environmental Modelling and Software", Burlington, USA.

Kralisch, S., Krause, P., Fink, M., Fischer, C., & Flügel, W.-A. (2007). Component based environmental modelling using the JAMS framework. In D. Kulasiri, & L. Oxley (Eds.), *Proceedings of the MODSIM 2007 international congress on modelling and simulation* (pp. 812–818). New Zealand: Christchurch.

Krause, P., (2001). Das hydrologische Modellsystem J2000: Beschreibung und anwendung in großen Flußeinzugsgebieten. Schriften des Forschungszentrum Jülich. Reihe Umwelt/Environment; Band 29.

Krause, P. (2002). Quantifying the impact of land use changes on the water balance of large catchments using the J2000 model. *Physics and Chemistry of the Earth*, *27*(9), 663–673.

Krause, P., Bende-Michl, U., Bäse, F., Fink, M., Flügel, W.-A., & Pfennig, B. (2006). Multiscale investigations in a mesoscale catchment hydrological modelling in the Gera catchment. *Advances in Geosciences*, *9*, 53–61.

Krause, P., Boyle, D. P., & Bäse, F. (2005). Comparison of different efficiency criteria for hydrological model assessment. *Advances in Geosciences*, *5*, 89–97.

Lutz, A. F., Immerzeel, W. W., Shrestha, A. B. & Bierkens, M. F. P. (2014). Consistent increase in High Asia's runoff due to increasing glacier melt and precipitation. *Nature Climate Change*, *4*(7), 587–592.

McCuen, R. (2005). The role of sensitivity analysis in hydrologic modelling. *Journal of Hydrology*, *18*, 37–53.

Merz, R., & Blöschl, G. (2004). Regionalisation of catchment model parameters. *Journal of Hydrology*, *287*, 95–123.

Moriasi, D. N., Arnold, J. G., Van Liew, M. W., Bingner, R. L., Harmel, R. D., & Veith, T. L. (2007). Model evaluation guidelines for systematic quantification of accuracy in watershed simulations. *Transactions of the ASABE*, *50*(3), 885–900.

Nepal, S. (2012). Evaluating upstream-downstream linkages of hydrological dynamics in the Himalayan Region. PhD. Thesis. Friedrich Schiller University of Jena, Jena.

Nepal, S. (2016). Impacts of climate change on the hydrological regime of the Koshi river basin in the Himalayan region. *Journal of Hydro-Environment Research*, *10*, 76–89.

Nepal, S., Krause, P., Flügel, W.-A., Fink, M., & Fischer, C. (2014). Understanding the hydrological system dynamics of a glaciated alpine catchment in the Himalayan region using the J2000 hydrological model. *Hydrological Processes*, *28*, 1329–1344.

Osti, R., & Egashira, S. (2009). Hydrodynamic characteristics of the Tam Pokhari glacial lake outburst flood in the Mt. Everest region, Nepal. *Hydrological Processes*, *23*(20), 2943–2955.

Patil, S., & Stieglitz, M. (2014). Modelling daily streamflow at ungauged catchments: What information is necessary? *Hydrological Processes*, *28*(3), 1159–1169.

Pfennig, B., Kipka, H., Wolf, M., Fink, M., Krause, P., & Flügel, W.-A. (2009). Development of an extended spatially distributed routing scheme and its impact on process oriented hydrological modelling results. IAHS Publ., 333, 37-43

Rees, H. G., Holmes, M. G. R., Young, A. R., & Kansakar, S. R. (2004). Recession-based hydrological models for estimating low flows in ungauged catchments in the Himalayas. *Hydrology and Earth System Sciences.*, *8*, 891–902.

Regmee, S. B., 2004. Water induced disasters in Nepal: Recent trends and measures. In: International Symposium on Utilization of Disaster Information, Organizing and Sharing Disaster Information in Asian Country, JSECE, Publication No. 44. The Japan Society of Erosion Control Engineering.

Rosero, E., Yang, Z.-L., Wagener, T., Gulden, L. E., Yatheendradas, S., & Niu, G.-Y. (2010). Quantifying parameter sensitivity, interaction, and transferability in hydrologically enhanced versions of the Noah land surface model over transition zones during the warm season. *J. Geophys. Res.*, *115*, D03106.

Shea, J. M., Immerzeel, W. W., Wagnon, P., Vincent, C., & Bajracharya, S. (2015). Modelling glacier change in the Everest region, Nepal Himalaya. *The Cryosphere*, *9*(3), 1105–1128.

Shrestha, S., Bastola, S., Babel, M. S., Dulal, K. N., Magome, J., Hapuarachchi, H. A. P., … Takeuchi, K. (2007). The assessment of spatial and temporal transferability of a physically based distributed hydrological model parameters in different physiographic regions of Nepal. *Journal of Hydrology*, *347*(1), 153–172.

Singh, R. D., Mishra, S. K., & Chowdhary, H. (2001). Regional flow-duration models for large number of ungauged Himalayan catchments for planning microhydro projects. *Journal of Hydrologic Engineering*, *6*(4), 310–316 Chicago.

Tasker, G. D. (1987). A comparison of methods for estimating low flow characteristics of streams. *Journal of the American Water Resources Association*, *23*, 1077–1083.

Wagnon, P., Vincent, C., Arnaud, Y., Berthier, E., Vuillermoz, E., Gruber, S., … Pokhrel, B. K. (2013). Seasonal and annual mass balances of Mera and Pokalde glaciers (Nepal Himalaya) since 2007. *The Cryosphere*, *7*(6), 1769–1786.

How to cite this article: Nepal S, Flügel W-A, Krause P, Fink M, Fischer C. Assessment of spatial transferability of process-based hydrological model parameters in two neighbouring catchments in the Himalayan Region. *Hydrological Processes*. 2017;1–15. https://doi.org/10.1002/hyp.11199